Electronic Supplementary Material (ESI) for Inorganic Chemistry Frontiers.
This journal is © the Partner Organisations 2023

ESI

$LaAeAl_3S_7$ (Ae = Ca, Sr): Cairo Pentagonal Layered thioaluminates Achieving Well-balance between Strong Second Harmonic Generation Response and Wide Bandgap

Jingjing Xu,[b] Kui Wu,[a,*] Bingbing Zhang,[b] Haohai Yu,[a,*] Huaijin Zhang[a,*]

[a] State Key Laboratory of Crystal Materials and Institute of Crystal Materials, Shandong University, Jinan, China

[b] College of Chemistry and Environmental Science, Hebei University, Baoding, China

E-mail: wukui@sdu.edu.cn; haohaiyu@sdu.edu.cn; huaijinzhang@sdu.edu.cn;

CONTENTS

1. Tables

Table S1. Dimensional distribution of AlS_4 units in the known thioaluminates.

Table S2. Comparison of the SHG effects and band gaps among $LaAeAl_3S_7$ and other reported NLO rare-earth chalcogenides.

Table S3. Crystal data and structure refinement for $LaAeAl_3S_7$.

Table S4. Comparison of the distortion degrees (Δd/‰) of AeS_8/$(La/Ae)S_8$ units among $LaAeAl_3S_7$ and $AeAl_2S_4$.

Table S1. Dimensional distribution of AlS_4 units in the known thioaluminates.

Compound	Space group	Unit	Dimensionality
$(Ag_{0.8}Cu_{3.2})Al_4S_8$	*I*-42*d*	AlS_4	3D
$(Ag_{3.6}Cu_{0.4})Al_4S_8$	*I*-42*d*	AlS_4	3D
Ln_3AlMS_7 (Ln=Y, Lanthanide series; M=Fe, Co, Ni, Zn, Mn, Cr, V, Ti)	$P6_3$	AlS_4	0D
Ba_2AlSbS_5	*Pnma*	AlS_4	0D
$LiBa_2AlS_4$	$P2_1/m$	AlS_4	0D
$Na_{0.80}Ba_{0.80}(AlS_3)_{0.80}$	*Pnma*	AlS_4	0D
$(Al_{0.973}Li_{3.126})S_3$	*C*2/*c*	AlS_4	0D
$Al(V_4S_8)$	*F*-43*m*	AlS_4	0D
Ag_9AlS_6	*F*-43*m*	AlS_4	0D
$Al_{0.55}Mo_2S_4$	F-43*m*	AlS_4	0D
$AlMo_4S_8$	F-43*m*	AlS_4	0D
$Al_{0.75}Mo_2S_4$	*F*-43*m*	AlS_4	0D
$Al(PS_4)$	*I*222	AlS_4	0D
$AlMo_4S_8$	*R*3*mR*	AlS_4	0D
$Na_5(AlS_4)$	*Pbca*	AlS_4	0D
$TaS_2Al_{0.33}$	$P6_3/mmc$	AlS_4	0D
Na_3AlS_3	$P2_1/n$	AlS_4	0D
$AlLi_5S_4$	$P2_1/m$	AlS_4	0D
$Na_6Al_2S_6$	$P2_1/c$	AlS_4	0D
$Rb_4(Al_2S_5)$	$Pna2_1$	AlS_4	1D
MAl_2S_4 (M=Eu, Pb, Sr)	*Cccm*	AlS_4	1D
$Bi_2(Al_4S_8)$	*P*4/*nncZ*	AlS_4	1D
$TlAlS_2$	*C*2/*c*	AlS_4	2D

$ZnAl_2S_4$	$Pna2_1$	AlS_4	2D
$FeAl_2S_4$	*R*3*mH*	AlS_4	2D
$MnAl_2S_4$	*R*3*mH*	AlS_4	2D
$AeAl_2S_4$ (Ae=Ca, Sr)	*Fddd*	AlS_4	2D
$Tl_3Al_{13}S_{21}$	*C*1*m*1	AlS_4	3D
$CuAlS_2$	*I*-42*d*	AlS_4	3D
$CdAl_2S_4$	*I*-4	AlS_4	3D
$HgAl_2S_4$	*I*-4	AlS_4	3D
$Tl_3(Al_7S_{12})$	$P2_1$	AlS_4	3D
$AlInS_3$	$P6_1$	AlS_4	3D
$BaAl_4S_7$	$Pmn2_1$	AlS_4	3D
$Ln_6Al_{3.3}S_{14}$ (Ln=Y, Lanthanide series)	$P6_3$	AlS_6; AlS_4	AlS_6 1D; AlS_4 0D

Table S2. Comparison of the SHG effect and band gap among $LaAeAl_3S_7$ and other reported NLO rare-earth chalcogenides.

Number	Compound	E_g (eV)	SHG (×$AgGaS_2$)	References
1	La_2CuSbS_5	2.06	0.5	S1
2	Sm_4InSbS_9	2.13	0.75	S2
3	$ZnY_8Si_2S_{14}$	2.38	0.84	S3
4	Gd_4GaSbS_9	2.41	0.8	S2
5	Dy_3GaS_6	2.81	0.084	S4
6	Y_3GaS_6	2.88	0.21	S4
7	La_3LiGeS_7	3.02	0.7	S5
8	$KYGeS_4$	3.15	1	S6
9	La_4InSbS_9	2.07	1.5	S7
10	$EuHgSnS_4$	2.14	1.77	S8
11	$La_8Sb_2S_{15}$	2.3	1.2	S9
12	La_3LiSnS_7	2.4	1.2	S5
13	$La_6In_2GeS_{14}$	2.61	1.8	S10
14	$Ba_4Sm_2Cd_3S_{10}$	2.77	1.8	S11
15	$LiSm_3SiS_7$	2.83	1.5	S5
16	$LaSrGa_3S_7$	2.92	1.3	S12
17	$LaCaGa_3S_7$	2.96	1.3	S12
18	$EuCdGeS_4$	2.5	2.6	S13
19	Sm_4GaSbS_9	2.23	3.8	S14
20	$La_6Ga_2GeS_{14}$	2.54	4.8	S10

21	$CsLaGeS_4$	3.6	0.18	S15
22	**$LaCaAl_3S_7$**	**3.76**	**0.8**	**this work**
23	**$LaSrAl_3S_7$**	**3.78**	**1.1**	**this work**

Table S3. Crystal data and structure refinement for $LaAeAl_3S_7$.

Empirical formula	$LaCaAl_3S_7$	$LaSrAl_3S_7$
Formula weight	484.35	531.89
crystal system	*Tetragonal*	
space group	*P*-42_1m	
a (Å)	9.4861(16)	9.5854(16)
c (Å)	6.1824(13)	6.2319(18)
Z, *V* (Å^3)	2, 556.3(2)	2, 572.6(3)
D_c (g/cm^3)	2.891	3.085
μ (mm^{-1})	5.788	9.784
GOF on F^2	1.063	1.059
R_1, wR_2 (I>2σ(I))^a	0.0399, 0.0941	0.0202, 0.0369
R_1, wR_2 (all data)	0.0442, 0.0968	0.0234, 0.0375
Flack parameter	-0.04(3)	0.039(14)
Largest diff. peak and hole (e Å^{-3})	1.463, -1.009	0.672, -0.320

Table S4. Comparison on the distortion degrees (Δd/‰) of AeS_8/$(La/Ae)S_8$ units among $LaAeAl_3S_7$ and $AeAl_2S_4$.

Compound	$(La/Ae)S_8$/AeS_8	$(La/Ae)S_8$/AeS_8 (Δd/‰)
$LaCaAl_3S_7$	$(La/Ca)S_8$	2.763
$LaSrAl_3S_7$	$(La/Sr)S_8$	3.062
	$Ca1S_8$	0.0007
$CaAl_2S_4$ (*Fddd*)	$Ca2S_8$	0.0024
	$Ca3S_8$	0.140
	$Sr1S_8$	0.030
$SrAl_2S_4$ (*Fddd*)	$Sr2S_8$	0.071
	$Sr3S_8$	0.092
$SrAl_2S_4$ (*Cccm*)	SrS_8	0.0073

2. Figures

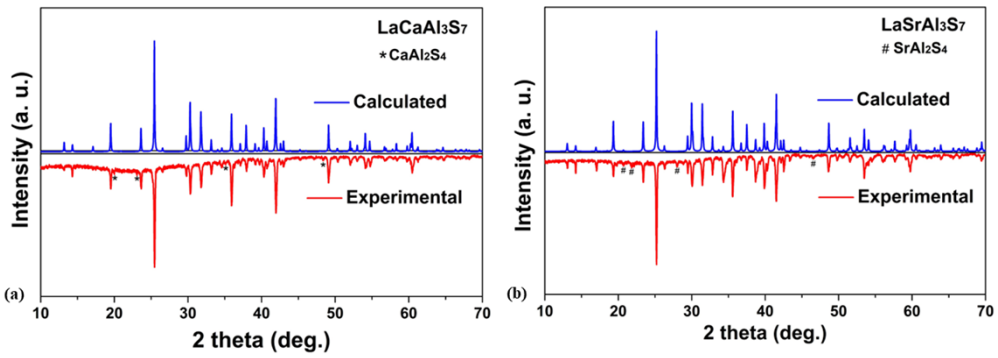

Fig. S1. Experimental XRD patterns for (a) $LaCaAl_3S_7$ and (b) $LaSrAl_3S_7$.

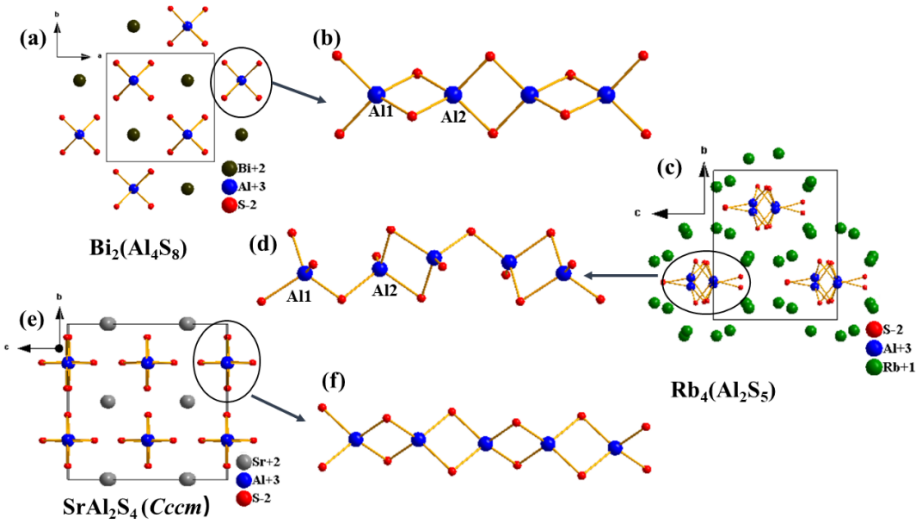

Fig. S2. (a) Crystal structure of $Bi_2(Al_4S_8)$ along the *c*-axis; (b) 1D chain is composed of AlS_4 units in $Bi_2(Al_4S_8)$; (c) Crystal structure of $Rb_4(Al_2S_5)$ along the *a*-axis; (d) 1D chain is composed of AlS_4 units in $Rb_4(Al_2S_5)$; (e) Crystal structure of $SrAl_2S_4$ along the *a*-axis; (f) 1D chain is composed of AlS_4 units in $SrAl_2S_4$.

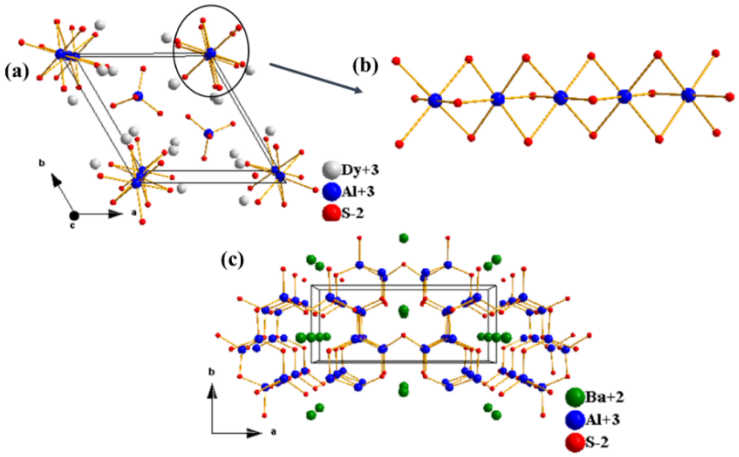

Fig. S3. (a) Crystal structure of $Dy_6Al_{3.3}S_{14}$ along the *c*-axis; (b) 1D chain is composed of AlS_6 units in $Dy_6Al_{3.3}S_{14}$; (c) Crystal structure of $BaAl_4S_7$ along the *c*-axis.

References

S1. H. Lin, Y. Li, M. Li, Z. Ma, L. Wu, X. Wu and Q. Zhu, Centric-to-acentric structure transformation induced by a stereochemically active lone pair: a new insight for design of IR nonlinear optical materials. *J. Mater. Chem. C*, 2019, **7**, 4638-4643.

S2. H. Zhao, Synthesis, crystal structure, and NLO property of the chiral sulfide Sm_4InSbS_9. *Z. Anorg. Allg. Chem.*, 2016, **642**, 56-59.

S3. S.-P. Guo, G.-C. Guo, M.-S. Wang, J.-P. Zou, G. Xu, G.-J. Wang, X.-F. Long and J.-S. Huang, A Series of New Infrared NLO Semiconductors, $ZnY_6Si_2S_{14}$, $Al_xDy_3(Si_yAl_{1-y})S_7$, and $Al_{0.33}Sm_3SiS_7$, *Inorg. chem.*, 2009, **48**, 7059-7065.

S4. M. J. Zhang, B. X. Li, B. W. Liu, Y. H. Fan, X. G. Li, H. Y. Zeng and G. C. Guo, Ln_3GaS_6 (Ln = Dy, Y): new infrared nonlinear optical materials with high laser induced damage thresholds, *Dalton Trans.*, 2013, **42**, 14223-14229.

S5. Y. Yang, Y. Chu, B. Zhang, K. Wu and S. Pan, Unique Unilateral-Chelated Mode-Induced d–p−π Interaction Enhances Second-Harmonic Generation Response in New Ln_3LiMS_7 Family, *Chem. Mater.*, 2021, **33**, 4225-4230.

S6. D. Mei, W. Cao, N. Wang, X. Jiang, J. Zhao, W. Wang, J. Dang, S. Zhang, Y. Wu, P. Rao and Z. Lin, Breaking through the "3.0 eV wall" of energy band gap in mid-infrared nonlinear optical rare earth chalcogenides by charge-transfer engineering, *Mater. Horiz.*, 2021, **8**, 2330-2334.

S7. H. J. Zhao, Y. F. Zhang and L. Chen, Strong Kleinman-forbidden second harmonic generation in chiral sulfide: La_4InSbS_9, *J. Am. Chem. Soc.*, 2012, **134**, 1993-1995.

S8. W. Xing, C. Tang, N. Wang, C. Li, Z. Li, J. Wu, Z. Lin, J. Yao, W. Yin and B. Kang, $EuHgGeSe_4$ and $EuHgSnS_4$: Two Quaternary Eu-Based Infrared Nonlinear Optical Materials with Strong Second-Harmonic-Generation Responses, *Inorg. Chem.*, 2020, **59**, 18452-18460.

S9. H. J. Zhao and L. J. Zhou, A Series of Noncentrosymmetric Antimony Sulfides $Ln_8Sb_2S_{15}$(Ln = La, Pr, Nd) – Syntheses, Crystal and Electronic Structures, and NLO Properties, *Eur. J. Inorg. Chem.*, 2015, **2015**, 964-968.

S10. Y.-F. Shi, Y.-k. Chen, M.-C. Chen, L.-M. Wu, H. Lin, L.-J. Zhou and L. Chen, Strongest Second Harmonic Generation in the Polar R_3MTQ_7 Family: Atomic Distribution Induced Nonlinear Optical Cooperation, *Chem. Mater.*, 2015, **27**, 1876-1884.

S11. Q. G. Yue, S. H. Zhou, B. Li, X. T. Wu, H. Lin and Q. L. Zhu, Quaternary Noncentrosymmetric Rare-Earth Sulfides $Ba_4RE_2Cd_3S_{10}$ (RE = Sm, Gd, or Tb): A Joint Experimental and Theoretical Investigation, *Inorg. Chem.*, 2022, **61**, 1797-1804.

S12. J. Xu, K. Wu, Y. Xiao, B. Zhang, H. Yu and H. Zhang, Mixed-Anion-Oriented Design of $LnMGa_3S_6O$ (Ln = La, Pr, and Nd; M = Ca and Sr) Nonlinear Optical Oxysulfides with Targeted Property Balance, *ACS Appl. Mater. Inter.*, 2022, **14**, 37967-37974

S13. W. Xing, N. Wang, Y. Guo, Z. Li, J. Tang, K. Kang, W. Yin, Z. Lin, J. Yao and B. Kang, Two rare-earth-based quaternary chalcogenides $EuCdGeQ_4$ (Q = S, Se) with strong second-harmonic generation, *Dalton Trans.*, 2019, **48**, 17620-17625.

S14. M.-C. Chen, L.-H. Li, Y.-B. Chen and L. Chen, In-phase alignments of asymmetric building units in Ln_4GaSbS_9 (Ln= Pr, Nd, Sm, Gd− Ho) and their strong nonlinear optical responses in middle IR, *J. Am. Chem. Soc.*, 2011, **133**, 4617-4624.

S15. M. Usman, M. D. Smith, G. Morrison, V. V. Klepov, W. Zhang, P. S. Halasyamani and H. C. Zur Loye, Molten Alkali Halide Flux Growth of an Extensive Family of Noncentrosymmetric Rare Earth Sulfides: Structure and Magnetic and Optical (SHG) Properties, *Inorg. Chem.*, 2019, **58**, 8541-8550.